Plants cope with fluctuating light by frequency-dependent nonphotochemical quenching and cyclic electron transport

Yuxi Niu[1] (iD), Dušan Lazár[2] (iD), Alfred R. Holzwarth[3] (iD), David M. Kramer[4] (iD), Shizue Matsubara[1] (iD), Fabio Fiorani[1] (iD), Hendrik Poorter[1,5] (iD), Silvia D. Schrey[1] (iD) and Ladislav Nedbal[1,2,6] (iD)

[1]Institute of Bio- and Geosciences/Plant Sciences, Forschungszentrum Jülich, Wilhelm-Johnen-Straße, D-52428, Jülich, Germany; [2]Department of Biophysics, Faculty of Science, Palacký University, Šlechtitelů 27, 783 71, Olomouc, Czech Republic; [3]Department of Physics and Astronomy, Faculty of Science, Vrije Universiteit Amsterdam, De Boelelaan 1105, NL-1081 HV, Amsterdam, the Netherlands; [4]MSU-DOE Plant Research Laboratory, Michigan State University, East Lansing, MI 48824, USA; [5]Department of Biological Sciences, Macquarie University, North Ryde, NSW, 2109, Australia; [6]PASTEUR, Department of Chemistry, École Normale Supérieure, Université PSL, Sorbonne Université, CNRS, 24, rue Lhomond, 75005, Paris, France

Author for correspondence:
Ladislav Nedbal
Email: *nedbal.lad@gmail.com*

Summary

- In natural environments, plants are exposed to rapidly changing light. Maintaining photosynthetic efficiency while avoiding photodamage requires equally rapid regulation of photoprotective mechanisms. We asked what the operation frequency range of regulation is in which plants can efficiently respond to varying light.
- Chlorophyll fluorescence, P700, plastocyanin, and ferredoxin responses of wild-types *Arabidopsis thaliana* were measured in oscillating light of various frequencies. We also investigated the *npq1* mutant lacking violaxanthin de-epoxidase, the *npq4* mutant lacking PsbS protein, and the mutants *crr2-2*, and *pgrl1ab* impaired in different pathways of the cyclic electron transport.
- The fastest was the PsbS-regulation responding to oscillation periods longer than 10 s. Processes involving violaxanthin de-epoxidase dampened changes in chlorophyll fluorescence in oscillation periods of 2 min or longer. Knocking out the PGR5/PGRL1 pathway strongly reduced variations of all monitored parameters, probably due to congestion in the electron transport. Incapacitating the NDH-like pathway only slightly changed the photosynthetic dynamics.
- Our observations are consistent with the hypothesis that nonphotochemical quenching in slow light oscillations involves violaxanthin de-epoxidase to produce, presumably, a largely stationary level of zeaxanthin. We interpret the observed dynamics of photosystem I components as being formed in slow light oscillations partially by thylakoid remodeling that modulates the redox rates.

Introduction

Plants grow in dynamic environments and can thrive also in rapidly fluctuating light (Muller *et al.*, 2001; Külheim *et al.*, 2002; Long *et al.*, 2022). Repeated filling and emptying of the biochemical pools in fluctuating light may cause damage by generating transient imbalances between tightly coupled redox reactions, potentially producing noxious reactive oxygen species (Pospíšil, 2009; Kono *et al.*, 2014; Kono & Terashima, 2014). Plants limit the damage and optimize their photosynthetic performance in fluctuating light by various regulatory mechanisms that operate with different activation and deactivation rates, which constrain the range of frequencies to which the regulation can effectively respond. Illustrative analogies are the range of audio frequencies that a human ear can hear or visible light range that the human eye can see. Here, we report on the limits of the operation range of photosynthetic nonphotochemical quenching and cyclic electron transport in the frequency domain.

Light fluctuations in nature may occur with a wide range of characteristic frequencies. Transient gaps in the upper canopy (Chazdon & Pearcy, 1991), wind-induced canopy movement (Peressotti *et al.*, 2001), and intermittent cloudiness (Knapp & Smith, 1987) give rise to irregular light patterns within canopies (Way & Pearcy, 2012; Smith & Berry, 2013; Kaiser *et al.*, 2018). According to the categorization of light fluctuations in canopy of higher plants established by Smith & Berry (2013), sunflecks were classified as light fluctuations with periods below 8 min, which is also the upper limit of periods investigated here. The short-period limit of 1 s of our experiments was dictated by the capacity of the used instrument to generate fast light oscillations.

Complex dynamic light changes occurring in natural environment can be simulated in laboratory by the Dynamic

Environmental Photosynthetic Imager (Cruz *et al.*, 2016). The forced oscillations methodology presented here uses a contrasting approach in which the response of plants is stimulated by a light that follows a single sinusoidal variation. The difference between investigating plant's response to complex light patterns and to single sinusoidal variation is analogous to probing absorption by a broadband and by monochromatic light. Such approaches reveal, in a different way, phenomena that do not appear under artificially static conditions and can thus identify photosynthetic processes important for dynamic responses. The method for investigating irregular or periodic stimulation has long been established in physics (Pintelon & Schoukens, 2012), and the used terminology is summarized here in Table 1. Based on universal and widely applied mathematical principles, random fluctuation of light can be reproduced as a superposition of harmonic functions, each determined by the period and amplitude of sinus and cosinus oscillations (Schwartz, 2008). If some of the characteristic elemental oscillations are, for example, too fast and thus outside of the operation range, then the photosynthetic regulation may be less effective. Similarly, when the operation range is reduced, for example, by a mutation, one can expect different dynamic responses in elemental oscillating light in the wild-type and in the mutant. The essentials of the frequency-domain analysis are summarized here in Supporting Information Notes S1 and in further detail available in Nedbal & Březina (2002), Nedbal *et al.* (2005), Nedbal & Lazár (2021), and Lazár *et al.* (2022). Nedbal & Lazár (2021) looked for the abrupt, qualitative changes in photosynthetic responses to oscillating light that would signal potential limits of operation frequency range in the green alga *Chlorella sorokiniana*. The experiments included light oscillations with periods ranging from 1 ms to 512 s and identified four frequency domains (α_1, β_1, α_2, and β_2), in which oxygenic photosynthesis of the alga exhibited contrasting dynamic features. In the two α domains, the amplitudes of the chlorophyll fluorescence (ChlF) oscillations were found to decrease in algae when the light oscillation was slower. The trend was opposite in the two β domains.

Due to an instrument limitation, a narrower range of light oscillations with periods between 1 s and 8 min was in our focus in this study on higher plants. Two major domains of contrasting dynamics were identified that are labeled here for simplicity without indices: α and β. Detailed measurements in the narrow range revealed an interesting dynamic behavior also in the α/β boundary.

Arabidopsis thaliana is exposed to fluctuating light due to intermittent cloudiness and canopy movements in monoculture as well as natural mixed plant communities (Mitchell-Olds, 2001; Pantazopoulou *et al.*, 2021). It is a model plant that represents well regulation in higher plants and is available with a wide range of well-defined mutations. We used elemental oscillating light with various periods to study its response to light fluctuations in the laboratory. Here, we focus on the responses of various components in the photosynthetic electron transport chain to fluctuating light (Fig. 1a), in particular, on nonphotochemical quenching (NPQ) and cyclic electron transport (CET) and their dynamics in fluctuating light (Holzwarth *et al.*, 2009;

Table 1 Explanation of technical terms.

Amplitude	The maximum deviation from a mean; in the case of harmonically modulated light, it is one-half of the difference between the light intensity maximum and minimum
Angular frequency ω	The parameter of light modulation or of plant response that defines how many times a full cycle (360° in angle degrees or 2π in radian units) is completed in a unit of time. It is related to the period T as: $\omega = \frac{2\pi}{T}$
Fluctuating light	Randomly changing light: its intensity pattern thus cannot be predicted
Forced oscillation	A repeating variation pattern of plant photosynthesis that is sustained in time by a *periodic* energy supply, here *harmonically modulated light*
Frequency-domain measurement	The measurement of plant activity applying *harmonically modulated light* with *period/ frequency* of the light modulation changing over a wide range; plant response(s) are measured as a function of the light modulation *frequency*
Harmonically modulated light	The light intensity that consists of a variable part that is changing as a harmonic function $a \times \sin\left(\frac{2\pi}{T} \cdot t\right) + b \times \cos\left(\frac{2\pi}{T} \cdot t\right)$ where t stands for time, T is the *period*, $\frac{2\pi}{T}$ the *angular frequency* of the light variation, and a, b are parameters that define together the *amplitude* and *phase* of the light modulation
Oscillation	A repeating variation pattern of light or plant activity
Period T	The time after which a process is repeated, here it applies both to the light modulation as well as to plant response elicited by the modulated excitation light
Periodic	Repeating
Oscillation phase	The parameter defining the progress of a periodic process: for example, phase 0 is the origin, the phase $\frac{1}{4} \cdot 2\pi$ represents one-quarter of the full cycle, phase 2π represents the full cycle
Resonance	A phenomenon of the increased *amplitude* of a measured response that occurs when the *frequency* of external forcing agrees with an internal characteristic *frequency* of the examined plant (sometimes called eigenfrequency)
Spontaneous oscillation	The *oscillation* of plant activities that sometimes appear in response to an abrupt change of external conditions; spontaneous oscillations of plants are fading over time
Time-domain measurement	The meaning common in fluorometry or spectroscopy of plants: the plant response to an aperiodic light change; mostly a stepwise dark-to-light or light-to-dark transition, often also the response to a short light flash measured as a function of time

Ruban, 2016; Yamamoto & Shikanai, 2019; Murchie & Ruban, 2020). The rapidly reversible component of NPQ protects the plant from transient excess light by sensing the high-light-induced acidification of the thylakoid lumen and reducing the flow of excitation energy to photosystem II (PSII) reaction centers (Demmig-Adams *et al.*, 2014; Ware *et al.*, 2015). This NPQ involves protonation of the PsbS protein (Li *et al.*, 2002;
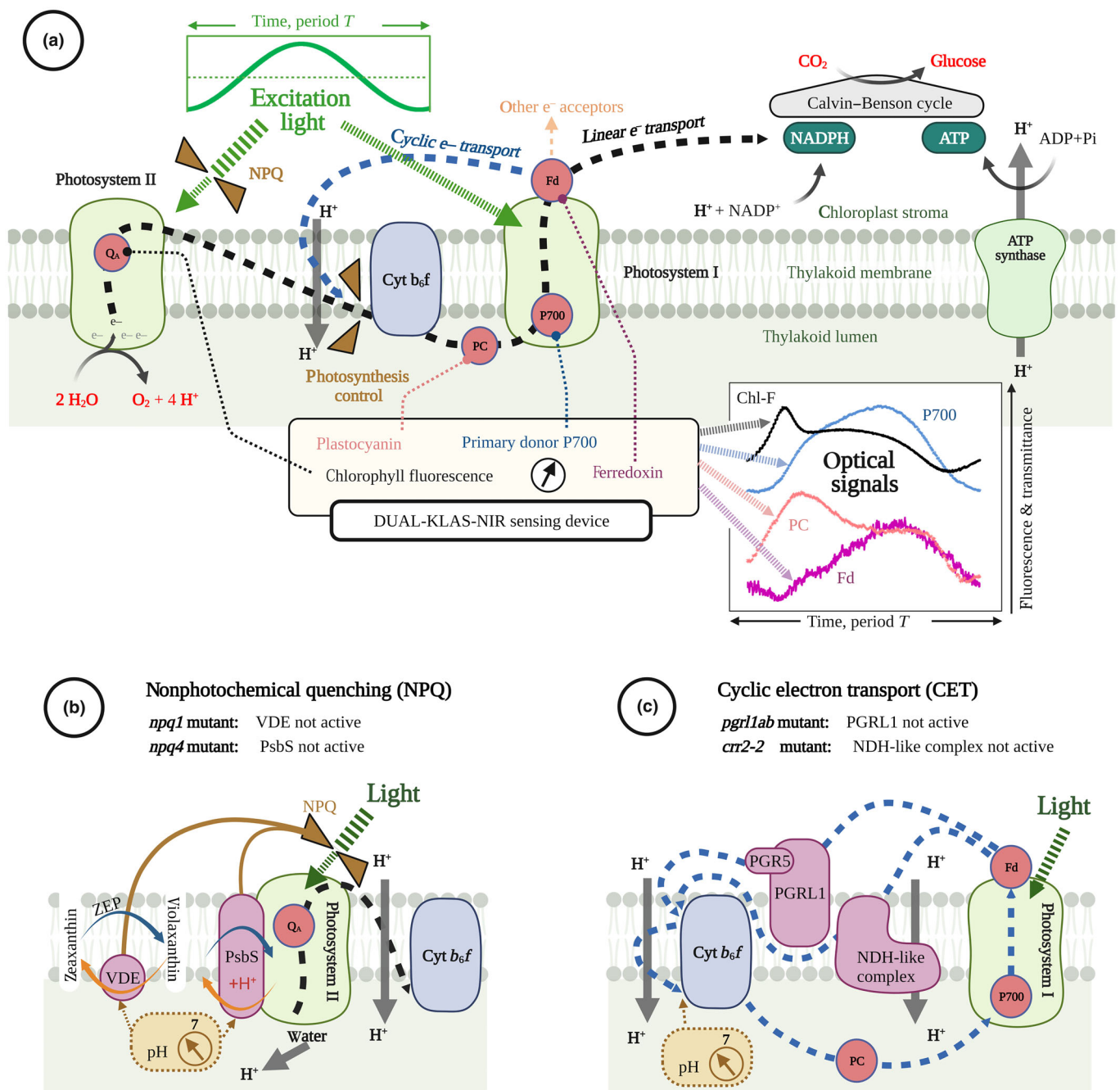
Fig. 1 Schematic diagram of proton-coupled electron transport of photosynthesis and associated photoprotective mechanisms. (a) A scheme of the photosynthetic apparatus in *Arabidopsis thaliana* showing the linear electron transport from water to $NADP^+$ by the black dashed line and the part of the cyclic electron transport around photosystem I (PSI) by the blue dashed line. The components that are monitored by the measured optical proxies (bottom right) were the Q_A redox state determining largely the chlorophyll fluorescence yield (ChlF), plastocyanin (PC), primary donor of PSI (P700), and ferredoxin (Fd). The lumen pH-controlled regulation of photosystem II (PSII) light harvesting efficiency (NPQ) and of the electron flow to cytochrome b_6f (Cyt b_6f) complex (photosynthesis control) are indicated by the brown valve symbol. The harmonically modulated light is represented by one period (green line top left). The optical signals measured (bottom right) by the Dual-KLAS-NIR instrument are described in the Materials and Methods section. (b) The violaxanthin deepoxidase (VDE) and PsbS protein constitute rapid nonphotochemical quenching mechanisms that are reducing the excitation of PSII. The zeaxanthin epoxidase (ZEP) is relaxing the quenching. Both processes are induced by low luminal pH. The cycles with blue- and orange-colored arrows represent transitions between low- and high-light states and back that occur periodically during the light oscillations. Orange arrows indicate NPQ induction processes, triggered by decreasing luminal pH, while blue arrows indicate the corresponding NPQ relaxation processes. (c) The cyclic electron transport proceeds by two parallel pathways: one via the Proton Gradient Regulation 5 (PGR5) and Proton Gradient Regulation-like 1 (PGRL1) complexes and the other via the NADH dehydrogenase-like complex (NDH-like) complex. The mutant *pgrl1ab* lacks PGR5/PGRL1-dependent pathway, whereas *crr2-2* lacks the pathway that depends on the NDH-like complex. Both CET pathways lower the luminal pH by the proton-coupled electron transport (Shikanai, 2014). In all schemes, the down-pointing gray arrows represent all processes leading to the accumulation of protons in the lumen relative to the stroma. The up-pointing gray arrow shows the dissipation of this pH difference by ATP synthase.

Roach & Krieger-Liszkay, 2012; Ruban, 2016) and the de-epoxidation of violaxanthin to zeaxanthin by the violaxanthin de-epoxidase enzyme (VDE; Fig. 1b; Gilmore, 1997; Jahns & Holzwarth, 2012). In fluctuating light, NPQ deficiency reduced plant's fitness (Külheim et al., 2002) while enhanced NPQ response caused higher photosynthetic efficiency and better growth (Kromdijk et al., 2016; De Souza et al., 2022). Kinetics of NPQ/xanthophyll cycle induction and relaxation in dark–light–dark transitions have been identified, for example, in Frommolt et al. (2001), Wehner et al. (2006), and Nilkens et al. (2010).

Cyclic electron transport mediates the electron transport from the reduced ferredoxin (Fd) at the acceptor side of photosystem I (PSI) via plastoquinone pool, cytochrome b_6f (Cyt b_6f) complex, and plastocyanin (PC) back to the donor side of PSI (Fig. 1c). By the proton-coupled electron transport, CET contributes to the proton motive force for ATP synthesis, thus adjusting the ATP : NADPH ratio for downstream carbon assimilation. The CET-induced lumen acidification also contributes to NPQ and regulates electron transport (Wang et al., 2015), protecting both PSII and PSI (Suorsa et al., 2012, 2013; Yamori et al., 2016; Shimakawa & Miyake, 2018; Nakano et al., 2019; Yamamoto & Shikanai, 2019). As in other angiosperms, A. thaliana plants possess two CET pathways (Shikanai, 2014). One involves the Proton Gradient Regulation 5 (PGR5) and Proton Gradient Regulation-like 1 (PGRL1) proteins (Munekage et al., 2002; DalCorso et al., 2008; Hertle et al., 2013; Sugimoto et al., 2013), whereas in the other, the electron is transported from Fd to plastoquinone via the NADH dehydrogenase-like complex (NDH-like; Fig. 1c; Yamamoto et al., 2011; Peltier et al., 2016). This latter pathway acidifies the thylakoid lumen not only by the plastoquinone/plastoquinol proton transport, but the NDH-like complex operates also as an energy-coupled proton pump (Kouřil et al., 2014; Strand et al., 2017; Laughlin et al., 2020). Fluctuating light damaged PSI in plants with a CET deficiency (Suorsa et al., 2012; Kono et al., 2014; Yamori et al., 2016) causing decreased photosynthesis control on the PSI donor side and reduced function of the PSI acceptor side (Yamamoto & Shikanai, 2019).

The first of the objectives of the present study was to identify the limiting frequencies at which the NPQ responds and beyond which it ceases responding, that is, to determine the NPQ operation range. In contrast to the response times obtained from activation during a dark-to-light induction, for example, in Wehner et al. (2006) and Nilkens et al. (2010), the limits of the NPQ operation range in oscillating light depend on an interplay of the activation and deactivation processes that both contribute to plant response to fluctuating light. Toward this goal, we explored the responses to oscillating light of the wild-type, the *npq1* mutant, which cannot convert violaxanthin into zeaxanthin by VDE (Niyogi et al., 1998), and of the *npq4* mutant that lacks the PsbS protein (Li et al., 2000).

The second objective was to discriminate between the roles played in an oscillating light by the two parallel pathways of CET. For this, we contrasted the *pgrl1ab* mutant that lacks the (PGR5/PGRL1)-dependent pathway (DalCorso et al., 2008),

and the *crr2-2* mutant impaired in the NDH-like complex-dependent pathway (Hashimoto et al., 2003) with their respective wild-types.

Understanding of the dynamics in complex systems like plants photosynthetic system requires simultaneous measurements of multiple system variables (Ganusov, 2016; Nedbal & Lazár, 2021) that would enable building robust mathematical models in the future (Kitano, 2001). *Toward this third objective*, we studied the dynamics of ChlF, and redox changes in P700, plastocyanin (PC), and ferredoxin (Fd) appearing in plants exposed to light that oscillated between light-limited and saturating intensities with periods changing between 1 s and 8 min. Two frequency domains and the boundary range between them were, in this way, characterized by highly contrasting dynamic behavior of NPQ and CET.

By characterizing the operational frequency ranges of the various processes by which plants protect themselves from dynamic changes in their light environment, we will better understand how plants utilize seemingly redundant regulatory processes to maintain the integrity of their photosynthetic machinery in such conditions, without compromising too much on their photosynthetic performance. This research provides the basis for development of novel frequency-domain methodologies and instruments in the field of plant science, which will reveal phenomena that do not appear under artificially static conditions.

Materials and Methods

Plant material and growth conditions

Arabidopsis thaliana (L.) Heynh. wild-type Col-0, trichome-lacking wild-type Col-gl1, and the mutants affected in NPQ (*npq1*, *npq4*) and in CET pathways (*pgrl1ab*, *crr2-2*) were used in the study. Col-0 was the background of the *npq1*, *npq4*, and *pgrl1ab* mutants, and the Col-gl1 was the background of *crr2-2*. The mutant *crr2-2* was kindly provided by Toshiharu Shikanai, Kyoto University, Japan, and *pgrl1ab* by Dario Leister, Ludwig Maximilian University München, Germany. Seeds were sown in commercial substrate (Pikier, Balster Einheitserdewerk, Fröndenberg, Germany). After 3 d of stratification in a 4°C dark room, the seedlings were transferred to a climate chamber with a light intensity of c. 100 µmol photons $m^{-2} s^{-1}$, 12 h : 12 h, light : dark photoperiod, 26°C : 20°C, day : night air temperature, and 60% relative air humidity. On the 15th day after sowing, the seedlings were transferred to 330 ml pots, one plant per pot filled with a commercial substrate (Lignostrat Dachgarten extensiv; HAWITA, Vechta, Germany). The environmental conditions in the climate chamber remained the same as for the seedlings. The plants were watered every day from the bottom to keep soil moisture approximately constant throughout the cultivation and during the experiments.

Chlorophyll fluorescence and KLAS-NIR measurements

In the sixth week after sowing, ChlF yield and redox changes of PC, P700, and Fd were measured simultaneously using a

Dual-KLAS-NIR spectrophotometer with a 3010 DUAL leaf cuvette (Heinz Walz GmbH, Effeltrich, Germany). Red actinic light (630 nm) was applied to both sides of the leaf. The pulse-amplitude-modulated green light (540 nm, 6 µmol photons m^{-2} s^{-1}) was applied to the abaxial side of the leaf to excite chlorophyll.

In addition to chlorophyll fluorescence yield, the Dual-KLAS-NIR allows to measure four dual-wavelength difference signals of transmittance simultaneously in the near-infrared part of the spectrum using 780–820, 820–870, 870–965, and 840–965 nm wavelength pairs (Klughammer & Schreiber, 2016; Schreiber & Klughammer, 2016). Four difference signals of transmittance can be deconvoluted into contributions corresponding dominantly to redox changes of Fd, primary donor of PSI (P700), and PC. The deconvolution relies on the selective differential transmittance spectra of P700, PC, and Fd for the four wavelength pairs, which were determined by the routine called Differential Model Plots (Klughammer & Schreiber, 2016; Schreiber & Klughammer, 2016). The plots were always constructed with two to three replicates. The Differential Model Plot was in this way determined for each genotype and used for the respective spectral deconvolution.

Plants were dark-acclimated overnight and then remained in darkness until their dynamic properties were investigated by the Dual-KLAS-NIR measurement with constant and oscillating actinic light, all at room temperature of 20°C, and in air of natural composition. The measurement started with the NIR-MAX routine on a dark-acclimated plant to estimate the maximum oxidation of PC and P700 (100%), and maximum reduction in Fd (−100%) as described in Klughammer & Schreiber (2016). The deconvolution of the overlapping optical transmission signals in near-infrared and the subsequent quantitative interpretation may, to some extent, be compromised by long measuring times, during which the initial deconvolution and min–max parameters may drift due to changing optical properties of the leaf. This would be of utmost importance in long conventional time-domain measurements that rely on stable reference signals, as time-domain measurements are difficult to correct for drift. With harmonically modulated light, one measures relative changes in the redox states of P700, PC, and Fd that are induced by oscillating light and this method is less sensitive to slowly drifting reference levels. The redox changes are quantified here relative to the value found at the trough of the oscillation, that is, when the light intensity reaches its minimum. The minimum photosynthetically active radiation (PAR) was always 100 µmol photons m^{-2} s^{-1}. By using a reference level taken in every oscillation period, we reduced or eliminated the influence of signal drift that may occur over long experimental periods. The dynamic trends occurring during the oscillations were, in this way, assessed using relative changes of the optical proxies named: apparent relative P700 and PC oxidation, and Fd reduction.

It is worth noting specific methodological aspects of the Fd signal. The implicit assumption of the NIR-MAX routine is that Fd is fully oxidized in darkness. This may not be always correct, because Fd can be reduced by multiple pathways, even in the absence of light. This potential caveat may result in an incorrect calibration of the optical proxy and in an apparent drift of the optical signal that is ascribed to fully oxidized Fd. In this situation, Fd reduction may exceed the expected range of 0% to −100%. Therefore, we shall not base any conclusions here on the absolute numerical values of the Fd-redox state but rather focus on trends in the Fd-reduction dynamics relative to the value found at the minimum PAR (100 µmol photons m^{-2} s^{-1}). Furthermore, it is worth noting that when the charge separation induced by light occurs in the PSI core complex, electron transfer from P700 to Fd occurs in a series of rapid redox reactions through A_0 (the monomeric form of Chl$a$) and A_1 (phylloquinone) to the [4Fe-4S] clusters (F_X, F_A, and F_B), and ultimately to Fd [2Fe-2S] (Schreiber & Klughammer, 2016). In the case of *in vivo* measurements, distinguishing the absorption changes of Fd from that of the other FeS proteins is practically impossible, as the NIR differential spectrum of F_A-F_B is similar to that of the Fd (Sétif *et al.*, 2019), and much larger absorption changes caused by other components can influence the signal deconvolution of different FeS proteins. Therefore, the 'Fd' signal used in this study is a mixture of signals of FeS components at the PSI acceptor side.

Actinic light protocols

Forced oscillations with changing frequencies Following induction in constant actinic light of 450 µmol photons m^{-2} s^{-1} (630 nm) that lasted 10 min, the plants were exposed to light that was oscillating around this level, between 100 and 800 µmol photons m^{-2} s^{-1}. The frequency (periods) and the number of periods of sinusoidal light were set in the KLAS-100 software (Heinz Walz GmbH). The periods were changing in a single continuous sequence: three periods of 8 min, five periods of each 4 min, 2 min, 1 min, 30 s, and 10 s, and finally 10 periods of 5 and 1 s (Notes S2; Fig. A). The order in which the periods were changing was not affecting our conclusions, and the same results were obtained when the periods were in an increasing sequence (Notes S3; Figs A–D). Three biological replicates of each *A. thaliana* genotype were examined.

Analysis of the signals induced by oscillating light The first period of 8 min oscillation was largely influenced by the transition from constant to oscillating light and the first two periods of the other oscillations were influenced by the change of light frequency. Because of these reasons, they were not analyzed (one example is offered in Notes S2; Fig. A). The later signals were already periodic and were used to extract the respective dynamic features by numeric analysis. The data representing each respective frequency in multiple replicated plants were averaged to improve the signal-to-noise ratio. The signal averages were then numerically approximated by a function *Fit*(*t*), consisting of a fundamental mode and of three upper harmonic modes as described in Nedbal & Lazár (2021):

$$Fit(t) = A_0 + A_1 \cdot \sin\left[1 \cdot \frac{2\pi(t-\tau_1)}{T}\right]$$
$$+ A_2 \cdot \sin\left[2 \cdot \frac{2\pi(t-\tau_2)}{T}\right] + A_3 \cdot \sin\left[3 \cdot \frac{2\pi(t-\tau_3)}{T}\right]$$
$$+ A_4 \cdot \sin\left[4 \cdot \frac{2\pi(t-\tau_4)}{T}\right].$$

Eqn 1

The least-square fitting procedure was done in MS EXCEL and the fit yielded the stationary component A_0, and the amplitudes and phase shifts $\{A_1, \tau_1\}$ for the fundamental harmonics, $\{A_2, \tau_2\}$, $\{A_3, \tau_3\}$, $\{A_4, \tau_4\}$ for the upper harmonic components. Typically, no more than two upper harmonics were needed as adding the third upper harmonic mode did not improve the chi-square of the fit. The fitted signals of P700, PC, and Fd apparent redox changes were normalized by subtracting by the signals obtained at the minimum light level (100 µmol photons m^{-2} s^{-1}) as explained above.

Results

Chlorophyll fluorescence emission

Eight different oscillation periods of light were sequentially applied to identify the characteristic frequency limits of NPQ and CET. Plants responded to the light changes by ChlF that was alternating in oscillations between minima and maxima around a stationary level A_0 (Eqn 1). Examples of raw data obtained with this protocol are shown in Notes S2; Fig. A. The information obtained in these experiments is condensed and represented by simple maximum–minimum differences and by the stationary component in Fig. 2.

The oscillatory ChlF component was calculated as the difference between the respective minimum and maximum of ChlF during one cycle. The stationary and oscillatory ChlF components (Fig. 2) were dependent on the frequency of light oscillations in three contrasting ways that can be categorized in the α (frequencies 1–1/10 s^{-1}) and β (frequencies 1/120–1/480 s^{-1}) domains, and α/β boundary domain whose frequencies 1/30 and 1/60 s^{-1} lead to a distinct resonance in ChlF (Notes S1; Fig. A). The corresponding periods were: 1–10 s in the α domain, 30–60 s in the α/β boundary domain, and 2–8 min in the β domain. The categorization of the frequency domains is compatible with that introduced for green algae in Nedbal & Lazár (2021).

The domain α included the shortest periods of light oscillations. Although the differences between the genotypes were large, the α domain can be defined by ChlF response remaining for each particular genotype largely the same, no matter if the period was 1, 5, or 10 s (Fig. 2). In the boundary α/β domain, the oscillatory ChlF component was typically higher than in the neighboring domains α and β (Fig. 2). This local maximum was reported earlier (Nedbal & Březina, 2002) and attributed to a resonance due to a regulatory feedback. This feature, pronounced in wild-types, was absent in the *npq4* PsbS-deficient mutant and

was damped, probably by electron transport limitation, in the *pgrl1ab* mutant (see arguments below).

One should note that the stationary component of ChlF does not exhibit the resonance feature in the α/β boundary domain. It is because the stationary component integrates effects of light that are averaged over many periods and are, thus, frequency independent.

Both the stationary and oscillatory components of the ChlF yield were increasing in the β domain in the *npq1*, *npq4*, and *pgrl1ab* mutants when the period increased from 2 to 8 min (Fig. 2). This trend was absent in wild-types and *crr2-2*.

The oscillatory components of ChlF in the α, α/β, and β domains are characterized in Fig. 2 only by the difference between the minima and maxima. These extremes often appear before or after the minima and maxima of light, and Fig. 2 does not show the respective phase shift of ChlF. We therefore present additional information about the phase shift of the ChlF extremes and further dynamic details in Fig. 3. This figure shows by a color code the entire dynamics of the oscillatory ChlF signal as it develops with the phase of the light oscillation along the abscissa axis and how it depends on the period of the oscillation along the ordinate axis. The ChlF signal was mostly more complex than a simple sinusoidal variation, containing also strong harmonic components with periods two or more times shorter than the period of the oscillating light. These components are called upper harmonics and are known from other oscillating systems, most illustratively from musical instruments where they determine the timbre. In plants, these upper harmonics are responsible for local rapid ChlF decreases in increasing light and vice versa or, in other words, for changes in ChlF response that are much faster than the changing light.

The changes in the ChlF yield in Fig. 3 were always induced by the same light pattern (top green line), oscillating between 100 and 800 µmol photons m^{-2} s^{-1}. The line shows the true light pattern that was slightly shifted in phase against the instrument protocol that aimed at generating the light minima at 0° and 360° and maximum at 180°. This instrumental deficiency had no impact on our conclusions.

The data show that both the stationary (Fig. 2) and the oscillatory part of the ChlF (Figs 2, 3) were strongly reduced in wild-type relative to the *npq1* and *npq4* mutants that lack VDE- and PsbS-dependent NPQ mechanisms, respectively. The most contrasting with wild-type was the *npq4* PsbS-deficient mutant exhibiting high amplitude ChlF variations that followed closely the light intensity suggesting dominance of photochemical quenching with little interference of NPQ. The ChlF was simply increasing due to reducing of the plastoquinone pool in increasing light and decreasing when the pool became more oxidized in the decreasing phase of the light oscillation. The amplitude of the ChlF oscillations in *npq4* was monotonously increasing from shorter to longer periods.

Unlike the *npq4* PsbS-deficient mutant, the *npq1* VDE-deficient mutant responded to the oscillating light with an overall phase-period pattern that was more complex than in *npq4* and not too different from wild-type (compare Fig. 3c with 3a). The ChlF yield maximum in the α/β boundary was found in both
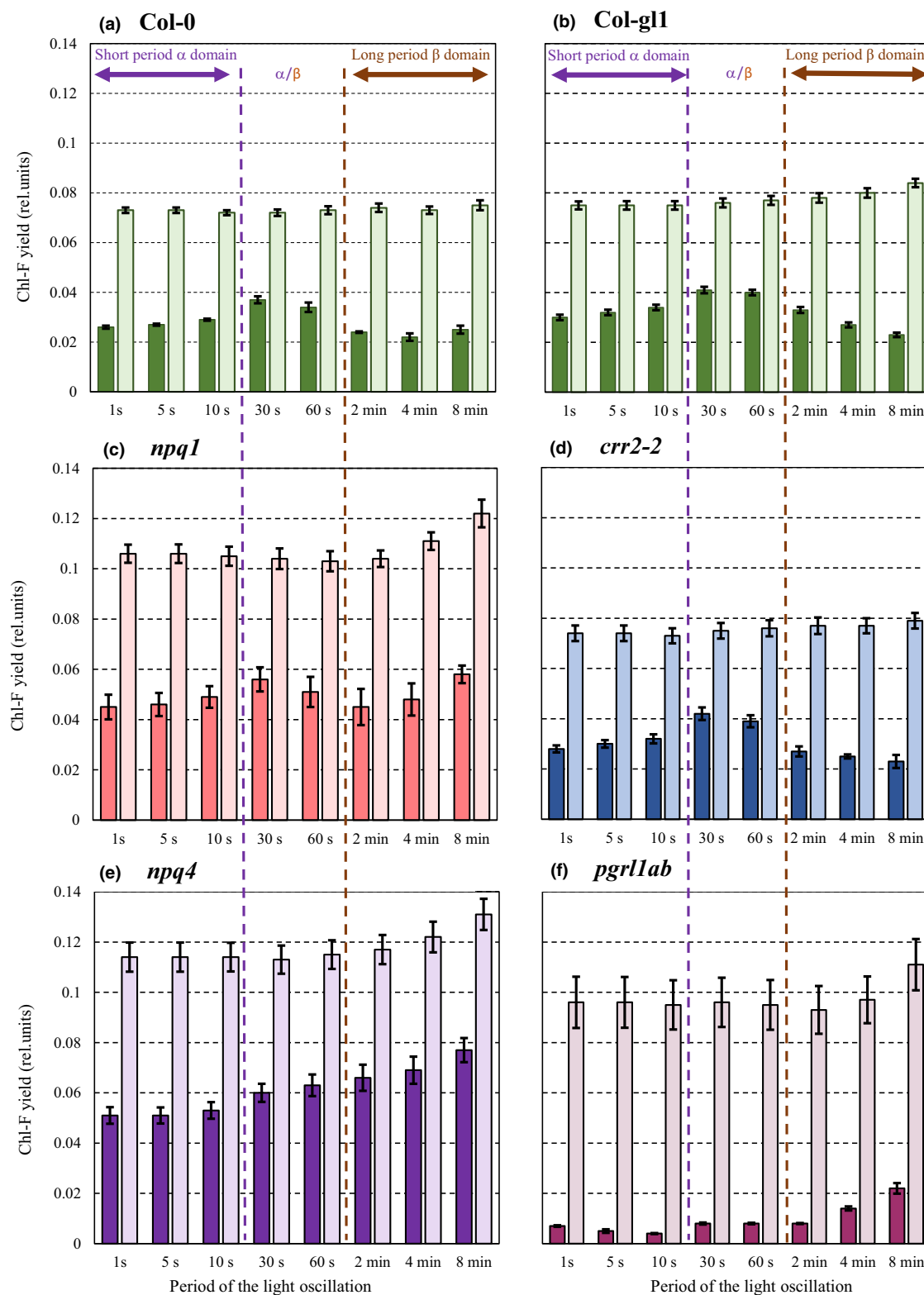
Fig. 2 Stationary (light-shaded) and oscillatory (dark-shaded) components of chlorophyll fluorescence (ChlF) yield measured in six genotypes of *Arabidopsis thaliana* ($n = 3$): (a) wild-type Col-0, (b) wild-type Col-gl1, (c) *npq1*, (d) *crr2-2*, (e) *npq4*, and (f) *pgrl1ab*. The actinic light was oscillating with short periods of 1, 5, and 10 s (α domain), with periods of 30 and 60 s (boundary α/β domain), and with long periods of 2, 4, and 8 min (β domain). The raw data from which this condensed information was extracted are shown in Supporting Information Notes S2; Fig. A. The oscillatory component was calculated as a difference between maximum and minimum of ChlF in one light period. The error bars represent SEs obtained from three biological replicates.
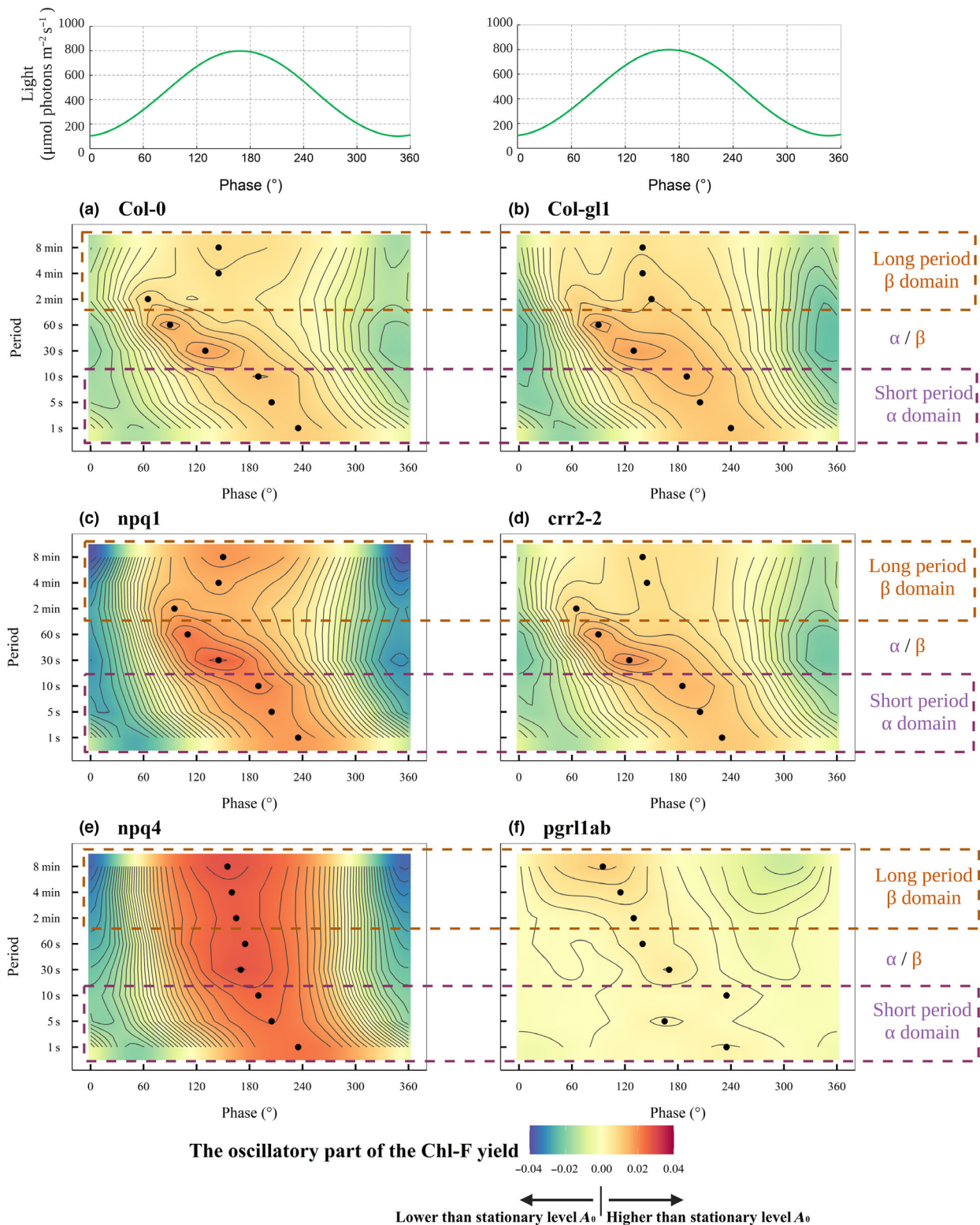
Fig. 3 Oscillatory part of the relative chlorophyll fluorescence (ChlF) yield. The green line in the upper panel represents light that was oscillating between 100 and 800 µmol photons m^{-2} s^{-1} with periods in the range of 1 s to 8 min. The progress of the light oscillation and ChlF response is shown by the phase between 0° and 360°, so that the abscissa is the same for all periods of oscillations that were applied. The other six panels show the oscillatory part of the ChlF yield induced in six genotypes of *Arabidopsis thaliana* ($n = 3$): (a) wild-type Col-0, (b) wild-type Col-gl1, (c) *npq1*, (d) *crr2-2*, (e) *npq4*, and (f) *pgrl1ab*. Blue colors indicate signals that were below the stationary ChlF yield, representing negative difference in the relative ChlF yield. Red colors represent oscillatory signals above the stationary ChlF yield. The black dots indicate the phase at which maximum ChlF yield at the given period occurred. The contour lines separate signal ranges of 0.0025 of relative units. The brown dashed rectangles indicate long periods of 2, 4, and 8 min (β domain), and the purple dashed rectangles indicate short periods of 1, 5, and 10 s (α domain).

npq1 and wild-type (Figs 2c, 3c). Only the amplitude of ChlF oscillations and the stationary ChlF component was higher in *npq1* than in wild-type, yet lower than in *npq4* (compare Fig. 2c with 2a and 2e). Another difference between *npq1* and wild-type was found when the period of the oscillating light increased from 60 s to 2 min and longer (β domain). When the periods increased from 2 to 8 min, the oscillatory part of the ChlF yield was largely quenched and not changing in the wild-type (Figs 2a, 3a) while it increased by *c.* 29% in the VDE-deficient *npq1* mutant (Figs 2c, 3c). We conclude that, in the light that was oscillating with increasingly long periods, the VDE-dependent NPQ in wild-type was able to respond, whereas ChlF oscillations appeared with increasing amplitudes in the VDE-deficient mutant. In contrast to this NPQ response, the stationary component of ChlF yield was quenched in the wild-type when compared to the *npq1* mutant to a level that was about the same in all tested periods (Fig. 2; Notes S4: Fig. A). We conclude that the VDE-dependent NPQ is largely responsible for protection in static or slowly changing light.

The distinct ChlF maximum in the α/β boundary found in all biological replicates of all genotypes that were competent in the PsbS-dependent NPQ mechanism, including wild-type and *npq1*, was suppressed in the *npq4* PsbS-deficient mutant. This PsbS-dependent resonance maximum occurred with the 30 s period in both wild-types at 130° phase, that is, *c.* 10.8 s after the light started rising from its minimum and, with the 60 s period, at 90° phase, that is, *c.* 15 s after the light minimum. The phase shift indicates that the plants and their PsbS-dependent NPQ mechanism required 10–20 s to change the trend from rising to declining ChlF in the ascending light phase. More on the resonance phenomenon is available in Notes S1: Figs A–C. This observed dynamics can be explained by the PsbS protein being necessary for rapid NPQ regulation in light that was oscillating with periods as short as 30 s.

A unique response to oscillating light was found in the *pgrl1ab* mutant that is impaired in the PGR5-PGRL1 pathway. The stationary part of ChlF was much less suppressed in *pgrl1ab* than in wild-types or in the *crr2-2* mutant (Fig. 2; Notes S4: Fig. A) while the variations around this stationary level that were caused by the light oscillations were by far smallest among all the tested genotypes (Fig. 3). The high stationary and low oscillatory ChlF components can signal congestion of the electron transport chain on the acceptor side of PSII. Unlike in wild-types and in the *crr2-2* mutant, the variations of ChlF yield in the *pgrl1ab* mutant exposed to long-period light oscillations (β) were stronger than in the short-period oscillations (α) indicating that NPQ became less effective when the periods were long. The dynamic features found in the *pgrl1ab* mutant cannot be attributed solely to impairment of one of the CET pathways. It is likely that the mutation impaired also the linear electron transport and affected induction of NPQ and photosynthesis control (DalCorso *et al.*, 2008; Suorsa *et al.*, 2016; Wada *et al.*, 2021).

The ChlF patterns found with the *crr2-2* mutant were like its wild-type (Figs 2, 3) suggesting that the response to oscillating light was only marginally affected by knocking out of the NDH-like complex-dependent pathway of CET.

Transmission proxies of PC, P700, and Fd-redox states

The frequency responses of apparent relative oxidation/reduction of P700 (Fig. 4), PC (Fig. 5), and Fd (Fig. 6) in oscillating light revealed diverging dynamics of components operating close to PSI. The P700 oxidation was, in all genotypes except the *pgrl1ab* mutant, closely following the oscillating light (Fig. 4). The amplitude of the P700 oscillations was relatively constant for periods shorter than 60 s (α and α/β) but increasing with long periods from 2 to 8 min (β). Compared with other genotypes tested, the *pgrl1ab* mutant showed qualitatively different frequency responses, in which the P700 redox state was largely independent of the oscillating light (Fig. 4f). This lack of variability of the P700 redox state signaled slowing or blockage of electron flow on the acceptor side of PSI in the *pgrl1ab* mutant (Shimakawa & Miyake, 2018). This presumed congestion in the linear electron transport may extend back to PSII and also explain the lack of variability of ChlF that was described above.

The frequency responses of the apparent relative PC oxidation (Fig. 5) depended strongly on the oscillation periods in all genotypes. In a rapidly oscillating light (α), PC was more oxidized in the high-light phase than around the light minima. Slow light oscillations (β) elicited a distinct phase dependence, in which PC was increasingly oxidized only in the first phase of the rising light. This trend was changed at a later ascending phase of the oscillation, when the PC oxidation dropped despite light still increasing and a saddle-type depression occurred around the light maximum.

The apparent relative Fd-redox states (Fig. 6) were, in wild-types and the *npq1* and *npq4* mutants, hardly changing between the light minima and light maxima of the rapid light oscillations (α). The NPQ limitations in the *npq1* and *npq4* mutants had only a minor effect on the redox state dynamics of the PSI primary donor P700 and on the PC and Fd dynamics. In the CET mutants, particularly in the *pgrl1ab* mutant, the apparent relative Fd proxy was signaling increasing reduction on the acceptor side of PSI in the strong light relative to the light minima. An apparent Fd reduction was occurring in the *crr2-2* mutant with the periods of 30 and 60 s, that is, in the α/β boundary (Fig. 6d), where the ChlF yield exhibited a resonance feature in all PsbS-competent genotypes including *crr2-2* (Fig. 3d). In the slow light oscillations (β), the apparent relative Fd proxy signaled a high oxidation on the acceptor side of PSI around the light maxima relative to light minima in all genotypes except the *pgrl1ab* mutant.

Discussion

The regulation of plant photosynthesis has its operating frequency range in which the contributing molecular mechanisms can function. This study employed harmonically oscillating light with different frequencies to identify the frequency limits of multiple photosynthetic regulatory processes. When the light oscillations exceed these limits being, for example, faster than the limit, the regulation responds only to the average of the light but cannot compensate for the rapidly changing light intensity. The transition at the limiting frequency of the operating range was
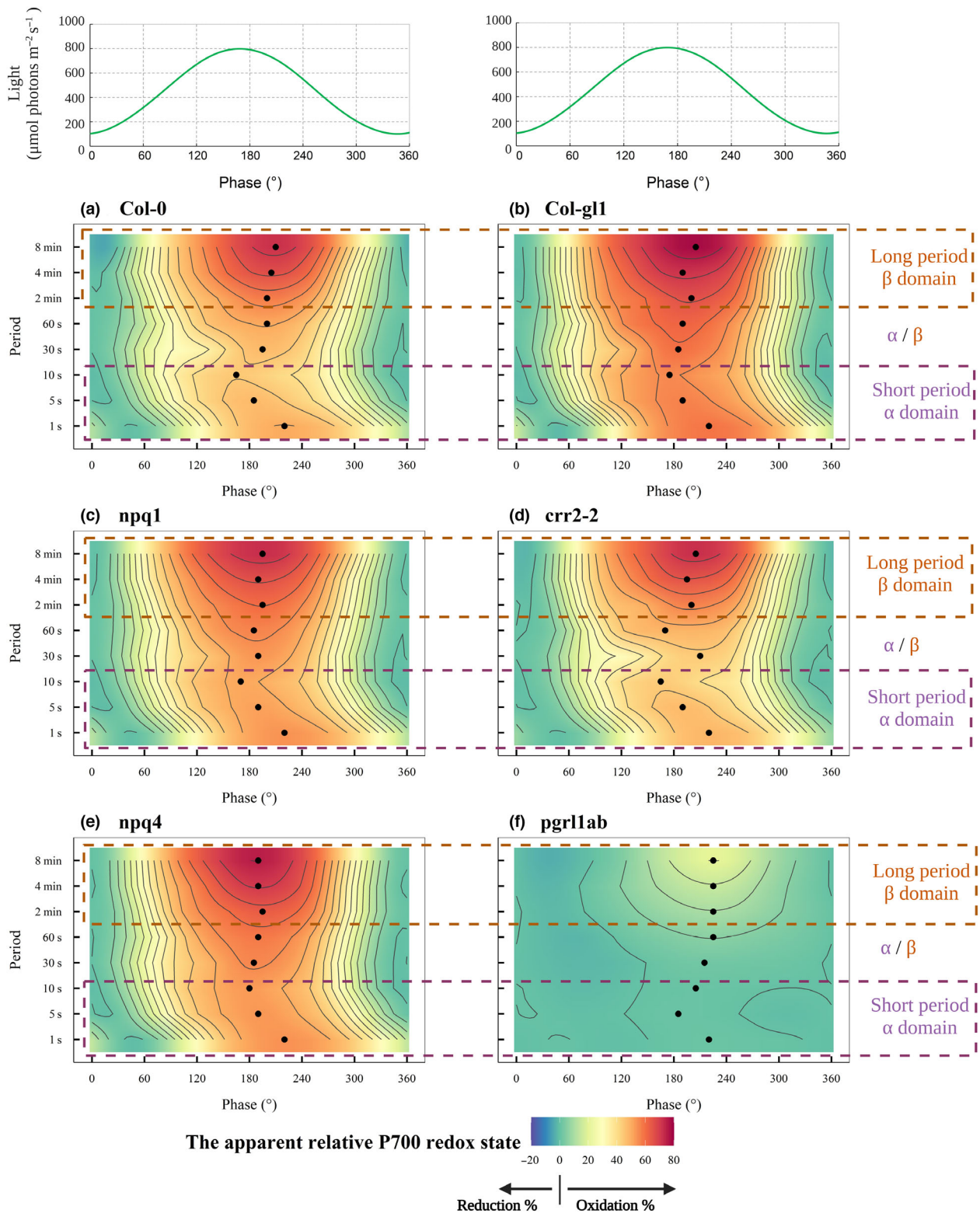
Fig. 4 Dynamics of primary donor of PSI (P700) in light that was oscillating as shown by the green line in the upper panels. The abscissa shows always the phase of the light oscillation. The six other panels show the apparent changes in the P700 redox state in six genotypes of *Arabidopsis thaliana* ($n = 3$): (a) wild-type Col-0, (b) wild-type Col-gl1, (c) *npq1*, (d) *crr2-2*, (e) *npq4*, and (f) *pgrl1ab*. The dynamics were induced by light oscillating between 100 and 800 µmol photons m^{-2} s^{-1} with periods in the range of 1 s to 8 min. The black dots indicate at which phase the maximum of the apparent P700 oxidation at a given period occurred. The color scale ranges from blue to red and represents the apparent oxidation of P700 relative to the state at minimum light level 100 µmol photons m^{-2} s^{-1} from low to high. Blue indicates that P700 was more reduced than at the light minimum, while red indicates that P700 was more oxidized than at the light minimum. The contour lines separate signal ranges of 5% of oxidation-reduction. The brown dashed rectangles indicate long periods of 2, 4, and 8 min (β domain), and the purple dashed rectangles indicate short periods of 1, 5, and 10 s (α domain).
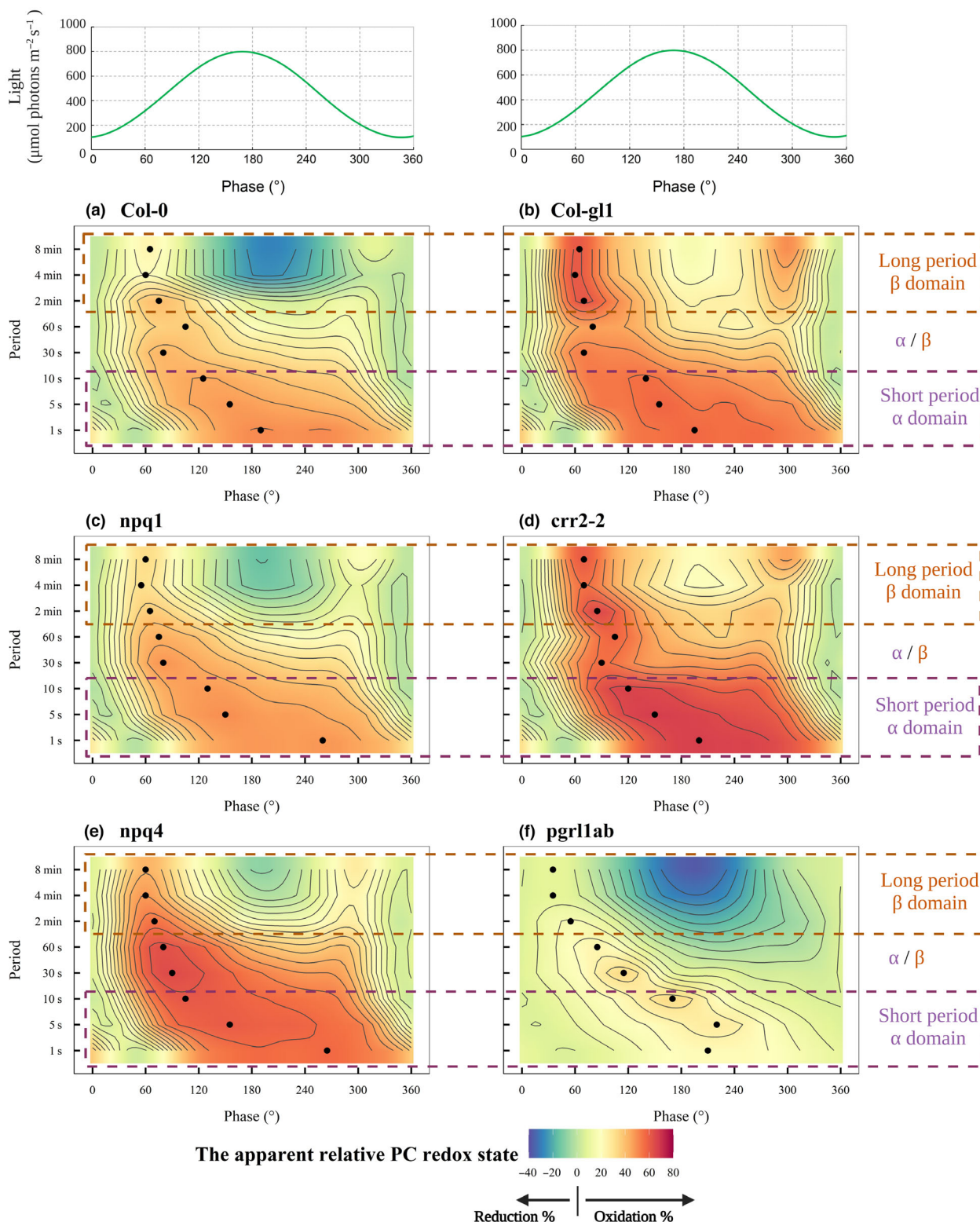
Fig. 5 Plastocyanin (PC) dynamics in light that was oscillating as shown by the green line in the upper panels. The abscissa shows always the phase of the light oscillation. The six other panels show the apparent changes in the PC redox state in six genotypes of *Arabidopsis thaliana* ($n = 3$): (a) wild-type Col-0, (b) wild-type Col-gl1, (c) *npq1*, (d) *crr2-2*, (e) *npq4*, and (f) *pgrl1ab*. The dynamics were induced by light oscillating between 100 and 800 µmol photons m^{-2} s^{-1} with periods in the range of 1 s to 8 min. The black dots indicate at which phase the maximum of the apparent PC oxidation at a given period occurred. The color scale ranges from blue to red and represents the apparent oxidation of PC relative to the state at minimum light level 100 µmol photons m^{-2} s^{-1} from low to high. Blue indicates that PC was more reduced than at the light minimum, while red indicates that PC was more oxidized than at the light minimum. The contour lines separate signal ranges of 5% of oxidation-reduction. The brown dashed rectangles indicate long periods of 2, 4, and 8 min (β domain), and the purple dashed rectangles indicate short periods of 1, 5, and 10 s (α domain).
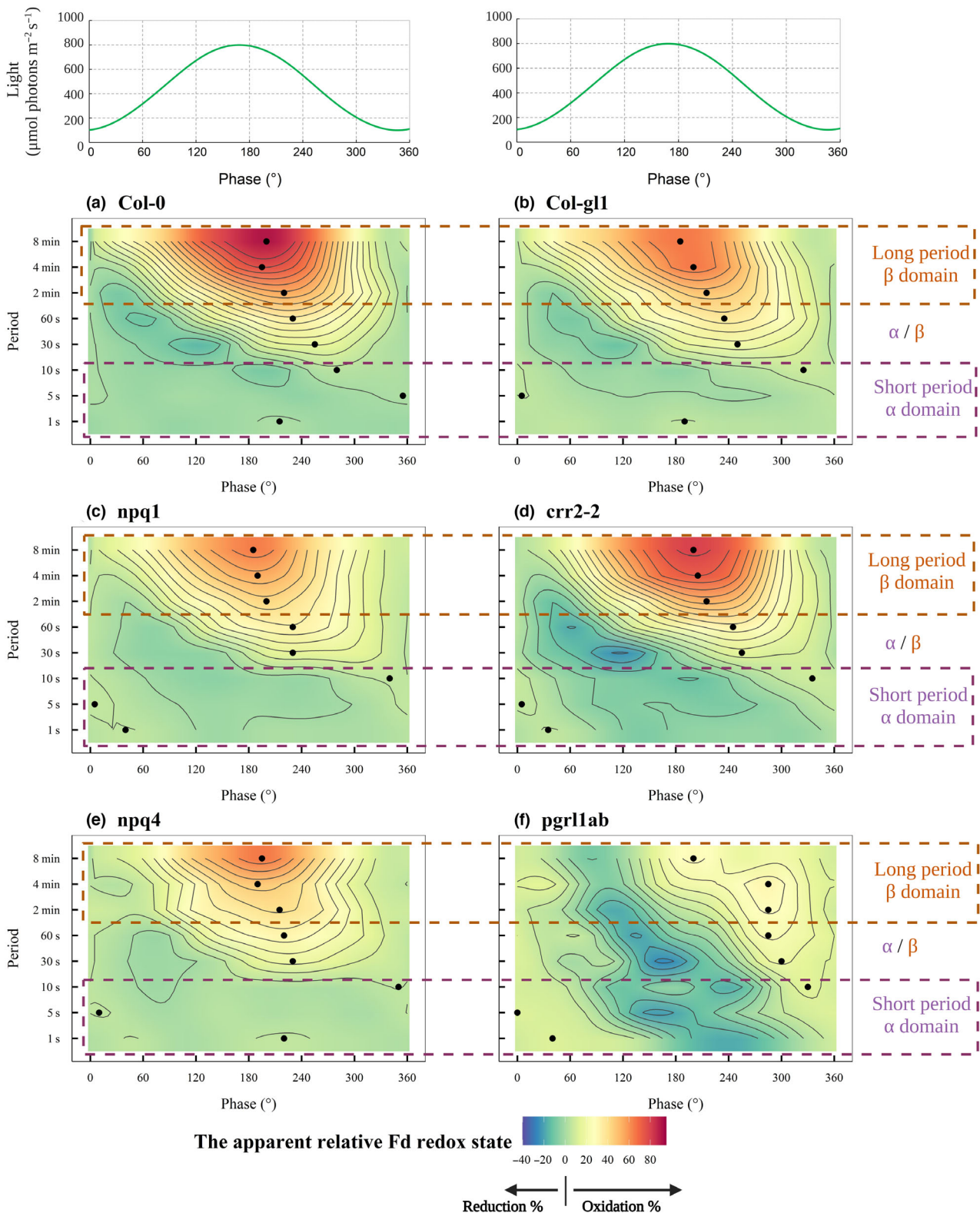
Fig. 6 The ferredoxin (Fd) dynamics in light that was oscillating as shown by the green line in the upper panels. The six other panels show the apparent changes in the Fd-redox state in six genotypes of *Arabidopsis thaliana* ($n = 3$): (a) wild-type Col-0, (b) wild-type Col-gl1, (c) *npq1*, (d) *crr2-2*, (e) *npq4*, and (f) *pgrl1ab*. The dynamics were induced by light oscillating between 100 and 800 μmol photons $m^{-2} s^{-1}$ with periods in the range of 1 s to 8 min. The black dots indicate at which phase the maximum of the apparent Fd oxidation at a given period occurred. The color scale ranges from blue to red and represents the apparent oxidation of Fd relative to the state at minimum light level 100 μmol photons $m^{-2} s^{-1}$ from low to high. Blue indicates that Fd was more reduced than at the light minimum, while red indicates that Fd was more oxidized than at the light minimum. The contour lines separate signal ranges of 5% of oxidation-reduction. The brown dashed rectangles indicate long periods of 2, 4, and 8 min (β domain), and the purple dashed rectangles indicate short periods of 1, 5, and 10 s (α domain).
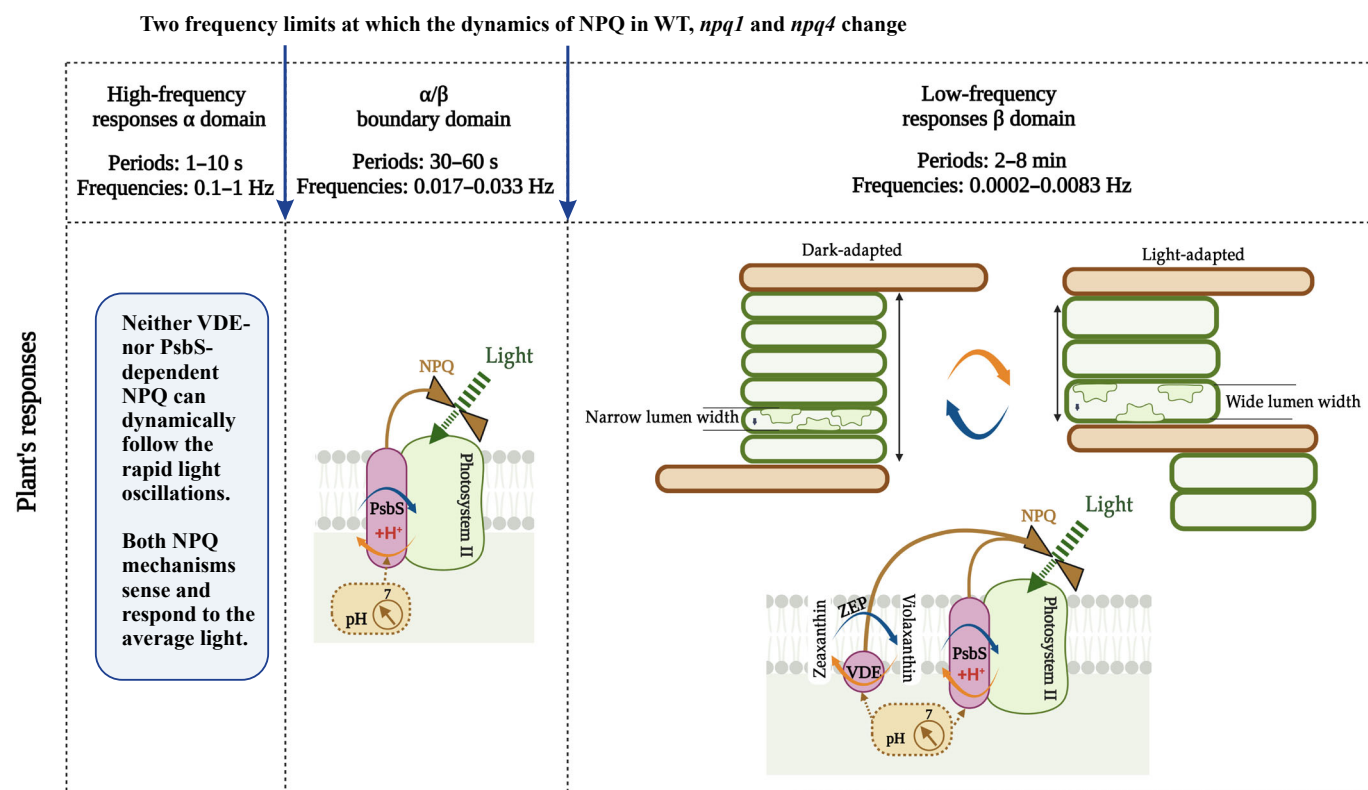
Two frequency limits at which the dynamics of NPQ in WT, *npq1* and *npq4* change

Fig. 7 Elemental harmonic components contributing to the natural fluctuations are classified into three frequency domains in which distinct dynamic responses occur (α, α/β, β). The scheme here represents a hypothesis that is proposed to explain the observed frequency responses of wild-types (WT) and *npq1* and *npq4* genotypes in these three domains. The nonphotochemical quenching (NPQ) response in the α/β boundary domain is proposed to be PsbS-dependent. The response to slow oscillations in the β domain is in addition formed also by violaxanthin de-epoxidase enzyme (VDE)-dependent NPQ that is tentatively proposed to occur with periodic reorganization of the thylakoid membrane. The dark- or low-light-adapted thylakoids are organized in large grana with narrow lumen space, reducing the area of contact between the grana membranes (green ellipses) and stromal lamellae (brown ellipses). With increasing the light intensity toward the maximum of the oscillation in our study, the thylakoids were proposed (Wood *et al*., 2018; Johnson & Wientjes, 2020) to be reorganized into numerous smaller grana, creating a larger area of contact between the grana membranes (green ellipses) and stromal lamellae (brown ellipses). Thylakoid lumen volume is proposed to expand with increasing light intensity and shrink when the light is decreasing (Kirchhoff *et al*., 2011). The lumen pH-controlled regulation of PSII light harvesting efficiency (NPQ) is indicated by the brown valve symbol. The cycles with blue- and orange-colored arrows represent transitions between low- and high-light states and back that may occur periodically during the light oscillations. Orange arrows indicate NPQ induction processes, triggered by decreasing luminal pH, while blue arrows indicate the corresponding NPQ relaxation processes. ZEP, zeaxanthin epoxidase.

manifested here by the changing dynamic response of plant photosynthesis, here ChlF, and the PC, P700, and Fd proxies, to light oscillations.

This work identified three types of plant responses that occurred in three frequency domains of light oscillations (α, α/β, β) that often occur in plant canopies. The three domains are separated from each other by two frequency limits that were identified here by qualitatively changing NPQ dynamics in wild-type and the *npq1* and *npq4* mutants (Fig. 3). This led us to formulate the hypotheses on two frequency limits of PsbS- and VDE-dependent NPQ that limit the operation range in natural fluctuating light: the first separating the domain α from α/β at *c.* $1/10-1/30 \, \text{s}^{-1}$ and the second between the domains α/β and β, by the separating limit at *c.* $1/60-1/120 \, \text{s}^{-1}$ (Fig. 7). The contrasting responses of the *crr2-2* and *pgrl1ab* CET mutants also supported the hypothesis that parallel pathways or mechanisms acting toward the

same function respond differently in the α, α/β, and β domains of the oscillating light.

Light oscillations in the α domain were too fast to be followed by NPQ

The light oscillations in the α domain were rapid and NPQ, being unable to follow the fast changes, responded mainly to the average irradiance. This static NPQ response reduced both stationary and oscillatory components of ChlF and was strongest in wild-type's that were competent both in the PsbS- and VDE-dependent quenching, and it was weakest in the *npq4* PsbS-deficient mutant. The PC, P700, and Fd proxies were also following the rapid light modulation in the α domain with a small delay which can be expected for the unregulated system of reactant pools that are filled and emptied by photosynthetic light reactions (Figs 4–6). The delay was larger for the faster light

oscillations indicating inertia of the pools. The only exception was the *pgrl1ab* mutant in which the electron transport was presumably congested, eliminating largely any variability (Shimakawa & Miyake, 2018).

Light frequencies in the boundary domain α/β elicited resonant enhancement of ChlF oscillations

The boundary α/β domain, represented here by the periods 30 and 60 s, was characterized by a crest maximum of ChlF that was found in plants competent in the PsbS-dependent NPQ and was absent in the *npq4* mutant missing PsbS (Li *et al.*, 2000). This dynamic feature can be assigned to the onset of the PsbS-dependent NPQ in light periods as short as 30 s. We propose that with these short periods, the VDE-dependent NPQ was unable to respond fast enough and the PsbS-dependent NPQ defined the plant's dynamic response in this domain alone (Fig. 7). The PsbS-dependent regulation activated in the α/β domain, marked by an increase in ChlF may thus be responsible for the resonance identified earlier (Nedbal & Březina, 2002) and also may play a role in the spontaneous oscillations in plants that also occur with a period *c.* 60 s (Delieu & Walker, 1983; Lazár *et al.*, 2005), that is, within the α/β domain. More on the resonance and spontaneous oscillations is available in Notes S1: Figs A–C. Despite the striking similarity between the resonance frequency and the frequency of spontaneous oscillations, involvement of PsbS-dependent regulation in the spontaneous oscillations of plants remains to be tested by future direct experiments that would also clarify if there were a synergy with activation of the Calvin–Benson cycle (Kaiser *et al.*, 2016; Graham *et al.*, 2017).

The slow light oscillations in the β domain permitted a complex plant response

The oscillatory component of the ChlF yield was in the β domain in wild-types strongly suppressed by PsbS- and VDE-dependent NPQ. The redox changes near PSI that were induced by slowly oscillating light occurred in wild-types, however, with high amplitudes despite the efficient NPQ. The contrast between the P700 and PC redox changes during the slow light oscillations (Figs 4, 5) was found also in the *crr2-2* and *pgrl1ab* mutants that were impaired in the CET pathways. We propose that the contrasting dynamic behavior of the PSI components might be caused by a periodic light-induced reorganization of the thylakoids that may differently affect PC and P700 (Ruban & Johnson, 2015; Ünnep *et al.*, 2017; Johnson & Wientjes, 2020; Li *et al.*, 2020; Hepworth *et al.*, 2021). Other alternative explanations for the observed slow changes could be the activation and deactivation of the Calvin–Benson cycle (Kaiser *et al.*, 2016; Graham *et al.*, 2017), malate valve (Thormählen *et al.*, 2017), chloroplast movements (Kihara *et al.*, 2020), or changing stomata conductance (Matthews *et al.*, 2018; Li *et al.*, 2021). The last two alternative mechanisms are however unlikely because we have not used blue light excitation that is known to elicit chloroplast movements and the light changes were in our experiments too fast to be

followed by the stomata aperture. Based on our results, slow light oscillations up to the period of 8 min are proposed to elicit periodic changes in PsbS- and VDE-dependent NPQ together with periodically changing thylakoid organization (Fig. 7). The effect of such a concerted regulation is small in the PsbS-impaired *npq4* mutant and limited in the VDE-impaired *npq1* mutant, indicating that PsbS, VDE, and thylakoid reorganization (Horton & Ruban, 2005) are required for fully functional regulation in the slowly oscillating light.

According to this model (Fig. 7), the PsbS-dependent NPQ plays an indispensable role in the plant's response to light that oscillates in the α/β and β domains. The *npq4* mutant impaired in this function will, in a natural fluctuating light with a range covering 30 s to 8 min, experience largely undamped oscillations in its electron transport chain and, most likely suffer from a dynamic load stress even though PAR may remain in the oscillations far below high levels that would cause photoinhibition in a static light.

On the complementarity of the time- and frequency-domain experiments

It is important to note that the widely explored dark-to-light induction yields information that is not equivalent to the information obtained from plant response to oscillating light or to natural fluctuating light. Namely, rate constants obtained in dark–light induction experiments may co-determine the frequency limits in a, potentially, complex way. The rate constant of antheraxanthin accumulation $1/130–1/260 \, s^{-1}$ reported in Wehner *et al.* (2006) for different lhcb complexes is not far from the lower frequency limit that we found separating the α/β domain from β ($1/60–1/120 \, s^{-1}$). Other work (Nilkens *et al.*, 2010) characterized the NPQ response by two characteristic time constants. In wild-type, they found a fast component with 70% relative contribution responding with a characteristic time of 60 s and a slower 30% component with 570 s. In mutant plants, the components were 50% and 50% and appeared with characteristic times of 460 and 2600 s in *npq4* and 9 and 1600 s in *npq1*. We underline however that the experimental protocol in Nilkens *et al.* (2010) is fundamentally different compared with ours because dark-to-light experiments map the entire transition of plants from neutral pH in lumen (no NPQ) to acidic pH in lumen (active NPQ). The oscillating light in our experiments, however, never dropped below $100 \, \mu$ mol photons $m^{-2} \, s^{-1}$ and pH in the thylakoid lumen was likely also oscillating in already acidic range and NPQ was already largely activated. The dynamic response of NPQ in our experiments reflected coupling of oscillating light and pH changes in the acidic range and further to activation and deactivation of molecular processes that involve PsbS and VDE and that control antenna excitation and, eventually, ChlF. One can further illustrate the difference between the rate constants measured in dark-to-light induction experiments and the frequency limits identified here using the VDE-dependent NPQ. The conventional time-domain induction experiments reveal dominantly the de-epoxidation of violaxanthin into antheraxanthin and

zeaxanthin, whereas the frequency limit found in the oscillating light would depend both on the de-epoxidation dominating in the rising light and the relatively slow epoxidation in the declining light. We propose that antheraxanthin and zeaxanthin produced during the preillumination and high-light phases of the oscillation did not significantly decline during the relatively short periods of low light during the oscillation. This could change in higher temperatures at or above 25°C when the epoxidation is faster (von Bismarck et al., 2023). Our hypothesis about stationary concentrations of antheraxanthin and zeaxanthin in fluctuating light needs to be further tested also by experiments in which the xanthophyll concentrations in the leaves would be directly measured during the light oscillation. The methodology described in Nilkens et al. (2010) cannot however be used for the range of periods applied here and, therefore, methods with a higher time resolution will need to be applied. This future development is required to test the hypothesis that the VDE-dependent oscillatory NPQ in the tested frequency range requires zeaxanthin or antheraxanthin to be present, but that the respective NPQ periodic changes are not caused directly by oscillating xanthophyll concentrations.

Outlook

Experiments using the KLAS-NIR spectrometer also revealed that the redox changes in and near PSI that were induced by oscillating light remained highly dynamic despite effective NPQ regulation in wild-type plants. The dynamic changes around PSI were largely independent of the mutations affecting NPQ. In the slow oscillation β domain, the dynamics of P700 were profoundly different from those of PC (Figs 4, 5). This may seem contradictory to the close interaction between the two redox components, with PC shuttling electrons from Cyt b_6f to P700. We propose that unlike P700 dynamics, the PC dynamics is modulated by a factor that connects both photosystems, such as photosynthesis control (Suorsa et al., 2013; Colombo et al., 2016; Johnson & Berry, 2021) and/or systemic properties such as changing thylakoid topology (Ünnep et al., 2017; Johnson & Wientjes, 2020; Li et al., 2020; Hepworth et al., 2021) that affects PC diffusion (Kirchhoff et al., 2011). The remodeling of the thylakoid membrane structure in slowly oscillating light may affect pronouncedly the heterogeneity of the plastoquinone pool and Cyt b_6f in granal and stromal segments of the thylakoid membranes (Joliot et al., 1992; Kirchhoff et al., 2000; Malone et al., 2021). The PQ pool in the grana thylakoid domains participates in the linear electron transport from PSII to Cyt b_6f, whereas the PQ pool in the stromal thylakoid domains serves primarily for CET (Fig. 1). Furthermore, one ought to consider that PC transports electrons from Cyt b_6f to P700 over long distance (Höhner et al., 2020), presumably with a low probability of backward electron transfer from P700 to PC and is subject to photosynthesis control (Johnson & Berry, 2021). The proposed effect of the thylakoid remodeling on the photosynthetic dynamics needs to be further examined because it may entail fundamental consequences for studies that are based on the dark-to-light transitions in the time domain. Unlike these traditional experimental protocols, the frequency-domain experiments employing oscillating light are applied to light-acclimated plants rather than to plants that change from dark-acclimated to light-acclimated state.

Identifying and quantifying frequency limits for operation of regulatory mechanisms and alternative pathways in plants exposed to oscillating light holds promise for improvements of photosynthetic efficiency in nature under fluctuating light. This may parallel the tremendous success of applying frequency-domain analysis in engineering and other fields of science (Ogata, 2010). At the molecular level, our work is broadly important in directly supporting the discovery of processes responsible for the regulation of photosynthetic electron fluxes and redox homeostasis in fluctuating light environments mimicking natural conditions. We also anticipate that at the leaf tissue level, new insights will be gained regarding the coupling of electron transfer with stomatal conductance and photosynthetic rates and the acclimation of these processes to fluctuating light environments (Matthews et al., 2018).

Based on these considerations, novel screening assays could be devised to characterize physiological manifestations of mutations and genetically diverse germplasm. These assays could detect altered metabolic control networks and support the identification of genetic mechanisms controlling dynamic responses to fluctuating environmental conditions. The potential applications of the methodologies presented here range from the integration in automated plant phenotyping platforms in controlled environments and glasshouses to the use in plant agro-ecological research through newly designed portable devices.

Competing interests

None declared.

Author contributions

YN, SM and LN planned and designed the research. YN performed experiments. YN, SDS and LN analyzed data. YN, DL, ARH, DMK, SM, SDS and LN interpreted the results. YN, DL, ARH, DMK, SM, FF, HP, SDS and LN wrote the manuscript.

ORCID

Fabio Fiorani https://orcid.org/0000-0001-8775-1541
Alfred R. Holzwarth https://orcid.org/0000-0002-9562-4873
David M. Kramer https://orcid.org/0000-0003-2181-6888
Dušan Lazár https://orcid.org/0000-0001-8035-4017
Shizue Matsubara https://orcid.org/0000-0002-1440-6496
Ladislav Nedbal https://orcid.org/0000-0002-4282-3406
Yuxi Niu https://orcid.org/0000-0002-9627-9864
Hendrik Poorter https://orcid.org/0000-0001-9900-2433
Silvia D. Schrey https://orcid.org/0000-0001-5821-1968

Data availability

Data are publicly available in the manuscript, and in the Supporting Information.

References

von Bismarck T, Korkmaz K, Ruß J, Skurk K, Kaiser E, Correa Galvis V, Cruz JA, Strand DD, Köhl K, Eirich J *et al.* **2023.** Light acclimation interacts with thylakoid ion transport to govern the dynamics of photosynthesis in Arabidopsis. *New Phytologist* 237: 160–176.

Chazdon RL, Pearcy RW. 1991. The importance of sunflecks for forest understory plants – photosynthetic machinery appears adapted to brief, unpredictable periods of radiation. *Bioscience* 41: 760–766.

Colombo M, Suorsa M, Rossi F, Ferrari R, Tadini L, Barbato R, Pesaresi P. 2016. Photosynthesis control: an underrated short-term regulatory mechanism essential for plant viability. *Plant Signaling & Behavior* 11: e1165382.

Cruz JA, Savage LJ, Zegarac R, Hall CC, Satoh-Cruz M, Davis GA, Kovac WK, Chen J, Kramer DM. 2016. Dynamic environmental photosynthetic imaging reveals emergent phenotypes. *Cell Systems* 2: 365–377.

DalCorso G, Pesaresi P, Masiero S, Aseeva E, Nemann DS, Finazzi G, Joliot P, Barbato R, Leister D. 2008. A complex containing PGRL1 and PGR5 is involved in the switch between linear and cyclic electron flow in Arabidopsis. *Cell* 132: 273–285.

De Souza AP, Burgess SJ, Doran L, Hansen J, Manukyan L, Maryn N, Gotarkar D, Leonelli L, Niyogi KK, Long SP. 2022. Soybean photosynthesis and crop yield are improved by accelerating recovery from photoprotection. *Science* 377: 541–854.

Delieu TJ, Walker DA. 1983. Simultaneous measurement of oxygen evolution and chlorophyll fluorescence from leaf pieces. *Plant Physiology* 73: 534–541.

Demmig-Adams B, Adams WW, Garab G, Govindjee G. 2014. *Non-photochemical quenching and energy dissipation in plants, algae and cyanobacteria preface.* Dordrecht, the Netherlands: Springer Netherlands.

Frommolt R, Goss R, Wilhelm C. 2001. The de-epoxidase and epoxidase reactions of *Mantoniella squamata* (Prasinophyceae) exhibit different substrate-specific reaction kinetics compared to spinach. *Planta* 213: 446–456.

Ganusov VV. 2016. Strong inference in mathematical modeling: a method for robust science in the twenty-first century. *Frontiers in Microbiology* 7: 1131.

Gilmore AM. 1997. Mechanistic aspects of xanthophyll cycle-dependent photoprotection in higher plant chloroplasts and leaves. *Physiologia Plantarum* 99: 197–209.

Graham PJ, Nguyen B, Burdyny T, Sinton D. 2017. A penalty on photosynthetic growth in fluctuating light. *Scientific Reports* 7: 12513.

Hashimoto M, Endo T, Peltier G, Tasaka M, Shikanai T. 2003. A nucleus-encoded factor, CRR2, is essential for the expression of chloroplast ndhB in Arabidopsis. *The Plant Journal* 36: 541–549.

Hepworth C, Wood WHJ, Emrich-Mills TZ, Proctor MS, Casson S, Johnson MP. 2021. Dynamic thylakoid stacking and state transitions work synergistically to avoid acceptor-side limitation of photosystem I. *Nature Plants* 7: 87–98.

Hertle AP, Blunder T, Wunder T, Pesaresi P, Pribil M, Armbruster U, Leister D. 2013. PGRL1 is the elusive ferredoxin-plastoquinone reductase in photosynthetic cyclic electron flow. *Molecular Cell* 49: 511–523.

Höhner R, Pribil M, Herbstová M, Lopez LS, Kunz HH, Li M, Wood M, Svoboda V, Puthiyaveetil S, Leister D *et al.* **2020.** Plastocyanin is the long-range electron carrier between photosystem II and photosystem I in plants. *Proceedings of the National Academy of Sciences, USA* 117: 15354–15362.

Holzwarth AR, Miloslavina Y, Nilkens M, Jahns P. 2009. Identification of two quenching sites active in the regulation of photosynthetic light-harvesting studied by time-resolved fluorescence. *Chemical Physics Letters* 483: 262–267.

Horton P, Ruban A. 2005. Molecular design of the photosystem II light-harvesting antenna: photosynthesis and photoprotection. *Journal of Experimental Botany* 56: 365–373.

Jahns P, Holzwarth AR. 2012. The role of the xanthophyll cycle and of lutein in photoprotection of photosystem II. *Biochimica et Biophysica Acta – Bioenergetics* 1817: 182–193.

Johnson JE, Berry JA. 2021. The role of cytochrome b$_6$f in the control of steady-state photosynthesis: a conceptual and quantitative model. *Photosynthesis Research* 148: 101–136.

Johnson MP, Wientjes E. 2020. The relevance of dynamic thylakoid organisation to photosynthetic regulation. *Biochimica et Biophysica Acta – Bioenergetics* 1861: 148039.

Joliot P, Lavergne J, Béal D. 1992. Plastoquinone compartmentation in chloroplasts. I. Evidence for domains with different rates of photo-reduction. *Biochimica et Biophysica Acta – Bioenergetics* 1101: 1–12.

Kaiser E, Morales A, Harbinson J. 2018. Fluctuating light takes crop photosynthesis on a rollercoaster ride. *Plant Physiology* 176: 977–989.

Kaiser E, Morales A, Harbinson J, Heuvelink E, Prinzenberg AE, Marcelis LF. 2016. Metabolic and diffusional limitations of photosynthesis in fluctuating irradiance in *Arabidopsis thaliana*. *Scientific Reports* 6: 31252.

Kihara M, Ushijima T, Yamagata Y, Tsuruda Y, Higa T, Abiko T, Kubo T, Wada M, Suetsugu N, Gotoh E. 2020. Light-induced chloroplast movements in *Oryza* species. *Journal of Plant Research* 133: 525–535.

Kirchhoff H, Hall C, Wood M, Herbstová M, Tsabari O, Nevo R, Charuvi D, Shimoni E, Reich Z. 2011. Dynamic control of protein diffusion within the granal thylakoid lumen. *Proceedings of the National Academy of Sciences, USA* 108: 20248–20253.

Kirchhoff H, Horstmann S, Weis E. 2000. Control of the photosynthetic electron transport by PQ diffusion microdomains in thylakoids of higher plants. *Biochimica et Biophysica Acta – Bioenergetics* 1459: 148–168.

Kitano H. 2001. *Foundations of systems biology.* Cambridge, MA, USA; London, UK: The MIT Press.

Klughammer C, Schreiber U. 2016. Deconvolution of ferredoxin, plastocyanin, and P700 transmittance changes in intact leaves with a new type of kinetic LED array spectrophotometer. *Photosynthesis Research* 128: 195–214.

Knapp AK, Smith WK. 1987. Stomatal and photosynthetic responses during sun/shade transitions in subalpine plants: influence on water use efficiency. *Oecologia* 74: 62–67.

Kono M, Noguchi K, Terashima I. 2014. Roles of the cyclic electron flow around PSI (CEF-PSI) and O$_2$-dependent alternative pathways in regulation of the photosynthetic electron flow in short-term fluctuating light in *Arabidopsis thaliana*. *Plant and Cell Physiology* 55: 990–1004.

Kono M, Terashima I. 2014. Long-term and short-term responses of the photosynthetic electron transport to fluctuating light. *Journal of Photochemistry and Photobiology B: Biology* 137: 89–99.

Kouřil R, Strouhal O, Nosek L, Lenobel R, Chamrád I, Boekema EJ, Šebela M, Ilík P. 2014. Structural characterization of a plant photosystem I and NAD(P) H dehydrogenase supercomplex. *The Plant Journal* 77: 568–576.

Kromdijk J, Głowacka K, Leonelli L, Gabilly ST, Iwai M, Niyogi KK, Long SP. 2016. Improving photosynthesis and crop productivity by accelerating recovery from photoprotection. *Science* 354: 587–860.

Külheim C, Ågren J, Jansson S. 2002. Rapid regulation of light harvesting and plant fitness in the field. *Science* 297: 91–93.

Laughlin TG, Savage DF, Davies KM. 2020. Recent advances on the structure and function of NDH-1: the complex I of oxygenic photosynthesis. *Biochimica et Biophysica Acta – Bioenergetics* **1861**: 148254.

Lazár D, Kaňa R, Klinkovský T, Nauš J. 2005. Experimental and theoretical study on high temperature induced changes in chlorophyll a fluorescence oscillations in barley leaves upon 2% CO_2. *Photosynthetica* **43**: 13–27.

Lazár D, Niu Y, Nedbal L. 2022. Insights on the regulation of photosynthesis in pea leaves exposed to oscillating light. *Journal of Experimental Botany* **73**: 6380–6393.

Li M, Mukhopadhyay R, Svoboda V, Oung HMO, Mullendore DL, Kirchhoff H. 2020. Measuring the dynamic response of the thylakoid architecture in plant leaves by electron microscopy. *Plant Direct* **4**: e00280.

Li TY, Shi Q, Sun H, Yue M, Zhang SB, Huang W. 2021. Diurnal response of photosystem I to fluctuating light is affected by stomatal conductance. *Cell* **10**: 3128.

Li X-P, Björkman O, Shih C, Grossman AR, Rosenquist M, Jansson S, Niyogi KK. 2000. A pigment-binding protein essential for regulation of photosynthetic light harvesting. *Nature* **403**: 391–395.

Li X-P, Gilmore AM, Niyogi KK. 2002. Molecular and global time-resolved analysis of a psbS gene dosage effect on pH- and xanthophyll cycle-dependent nonphotochemical quenching in photosystem II. *Journal of Biological Chemistry* **277**: 33590–33597.

Long SP, Taylor SH, Burgess SJ, Carmo-Silva E, Lawson T, De Souza AP, Leonelli L, Wang Y. 2022. Into the shadows and back into sunlight: photosynthesis in fluctuating light. *Annual Review of Plant Biology* **73**: 617–648.

Malone LA, Proctor MS, Hitchcock A, Hunter CN, Johnson MP. 2021. Cytochrome b_6f – orchestrator of photosynthetic electron transfer. *Biochimica et Biophysica Acta – Bioenergetics* **1862**: 148380.

Matthews JSA, Vialet-Chabrand S, Lawson T. 2018. Acclimation to fluctuating light impacts the rapidity of response and diurnal rhythm of stomatal conductance. *Plant Physiology* **176**: 1939–1951.

Mitchell-Olds T. 2001. *Arabidopsis thaliana* and its wild relatives: a model system for ecology and evolution. *Trends in Ecology & Evolution* **16**: 693–700.

Muller P, Li XP, Niyogi KK. 2001. Non-photochemical quenching. A response to excess light energy. *Plant Physiology* **125**: 1558–1566.

Munekage Y, Hojo M, Meurer J, Endo T, Tasaka M, Shikanai T. 2002. PGR5 is involved in cyclic electron flow around photosystem I and is essential for photoprotection in Arabidopsis. *Cell* **110**: 361–371.

Murchie EH, Ruban AV. 2020. Dynamic non-photochemical quenching in plants: from molecular mechanism to productivity. *The Plant Journal* **101**: 885–896.

Nakano H, Yamamoto H, Shikanai T. 2019. Contribution of NDH-dependent cyclic electron transport around photosystem I to the generation of proton motive force in the weak mutant allele of pgr5. *Biochimica et Biophysica Acta – Bioenergetics* **1860**: 369–374.

Nedbal L, Březina V. 2002. Complex metabolic oscillations in plants forced by harmonic irradiance. *Biophysical Journal* **83**: 2180–2189.

Nedbal L, Březina V, Červený J, Trtílek M. 2005. Photosynthesis in dynamic light: systems biology of unconventional chlorophyll fluorescence transients in *Synechocystis* sp. PCC 6803. *Photosynthesis Research* **84**: 99–106.

Nedbal L, Lazár D. 2021. Photosynthesis dynamics and regulation sensed in the frequency domain. *Plant Physiology* **187**: 646–661.

Nilkens M, Kress E, Lambrev P, Miloslavina Y, Muller M, Holzwarth AR, Jahns P. 2010. Identification of a slowly inducible zeaxanthin-dependent component of non-photochemical quenching of chlorophyll fluorescence generated under steady-state conditions in Arabidopsis. *Biochimica et Biophysica Acta – Bioenergetics* **1797**: 466–475.

Niyogi KK, Grossman AR, Björkman O. 1998. Arabidopsis mutants define a central role for the xanthophyll cycle in the regulation of photosynthetic energy conversion. *Plant Cell* **10**: 1121–1134.

Ogata K. 2010. *Modern control engineering*. Boston, MA, USA: Prentice-Hall.

Pantazopoulou CK, Bongers FJ, Pierik R. 2021. Reducing shade avoidance can improve Arabidopsis canopy performance against competitors. *Plant, Cell & Environment* **44**: 1130–1141.

Peltier G, Aro EM, Shikanai T. 2016. NDH-1 and NDH-2 plastoquinone reductases in oxygenic photosynthesis. *Annual Review of Plant Biology* **67**: 55–80.

Peressotti A, Marchiol L, Zerbi G. 2001. Photosynthetic photon flux density and sunfleck regime within canopies of wheat, sunflower and maize in different wind conditions. *Italian Journal of Agronomy* **4**: 87–92.

Pintelon R, Schoukens J. 2012. *System identification: a frequency domain approach*. Hoboken, NJ, USA: John Wiley & Sons.

Pospíšil P. 2009. Production of reactive oxygen species by photosystem II. *Biochimica et Biophysica Acta – Bioenergetics* **1787**: 1151–1160.

Roach T, Krieger-Liszkay A. 2012. The role of the PsbS protein in the protection of photosystems I and II against high light in *Arabidopsis thaliana*. *Biochimica et Biophysica Acta – Bioenergetics* **1817**: 2158–2165.

Ruban AV. 2016. Nonphotochemical chlorophyll fluorescence quenching: mechanism and effectiveness in protecting plants from photodamage. *Plant Physiology* **170**: 1903–1916.

Ruban AV, Johnson MP. 2015. Visualizing the dynamic structure of the plant photosynthetic membrane. *Nature Plants* **1**: 15161.

Schreiber U, Klughammer C. 2016. Analysis of photosystem I donor and acceptor sides with a new type of online-deconvoluting kinetic LED-array spectrophotometer. *Plant and Cell Physiology* **57**: 1454–1467.

Schwartz L. 2008. *Mathematics for the physical sciences*. Mineola, NY, USA: Courier Dover.

Sétif P, Boussac A, Krieger-Liszkay A. 2019. Near-infrared *in vitro* measurements of photosystem I cofactors and electron-transfer partners with a recently developed spectrophotometer. *Photosynthesis Research* **142**: 307–319.

Shikanai T. 2014. Central role of cyclic electron transport around photosystem I in the regulation of photosynthesis. *Current Opinion in Biotechnology* **26**: 25–30.

Shimakawa G, Miyake C. 2018. Changing frequency of fluctuating light reveals the molecular mechanism for P700 oxidation in plant leaves. *Plant Direct* **2**: e00073.

Smith WK, Berry ZC. 2013. Sunflecks? *Tree Physiology* **33**: 233–237.

Strand DD, Fisher N, Kramer DM. 2017. The higher plant plastid NAD(P)H dehydrogenase-like complex (NDH) is a high efficiency proton pump that increases ATP production by cyclic electron flow. *Journal of Biological Chemistry* **292**: 11850–11860.

Sugimoto K, Okegawa Y, Tohri A, Long TA, Covert SF, Hisabori T, Shikanai T. 2013. A single amino acid alteration in PGR5 confers resistance to antimycin A in cyclic electron transport around PSI. *Plant and Cell Physiology* **54**: 1525–1534.

Suorsa M, Grieco M, Jarvi S, Gollan PJ, Kangasjarvi S, Tikkanen M, Aro EM. 2013. PGR5 ensures photosynthetic control to safeguard photosystem I under fluctuating light conditions. *Plant Signaling & Behavior* **8**: e22741.

Suorsa M, Järvi S, Grieco M, Nurmi M, Pietrzykowska M, Rantala M, Kangasjärvi S, Paakkarinen V, Tikkanen M, Jansson S *et al.* 2012. PROTON GRADIENT REGULATION5 is essential for proper acclimation of Arabidopsis photosystem I to naturally and artificially fluctuating light conditions. *Plant Cell* **24**: 2934–2948.

Suorsa M, Rossi F, Tadini L, Labs M, Colombo M, Jahns P, Kater Martin M, Leister D, Finazzi G, Aro E-M *et al.* 2016. PGR5-PGRL1-dependent cyclic electron transport modulates linear electron transport rate in *Arabidopsis thaliana*. *Molecular Plant* **9**: 271–288.

Thormählen I, Zupok A, Rescher J, Leger J, Weissenberger S, Groysman J, Orwat A, Chatel-Innocenti G, Issakidis-Bourguet E, Armbruster U *et al.* 2017. Thioredoxins play a crucial role in dynamic acclimation of photosynthesis in fluctuating light. *Molecular Plant* **10**: 168–182.

Ünnep R, Zsiros O, Hörcsik Z, Markó M, Jajoo A, Kohlbrecher J, Garab G, Nagy G. 2017. Low-pH induced reversible reorganizations of chloroplast thylakoid membranes – as revealed by small-angle neutron scattering. *Biochimica et Biophysica Acta – Bioenergetics* **1858**: 360–365.

Wada S, Amako K, Miyake C. 2021. Identification of a novel mutation exacerbated the PSI photoinhibition in pgr5/pgrl1 mutants; caution for overestimation of the phenotypes in Arabidopsis pgr5-1 mutant. *Cells* **10**: 2884.

Wang CJ, Yamamoto H, Shikanai T. 2015. Role of cyclic electron transport around photosystem I in regulating proton motive force. *Biochimica et Biophysica Acta – Bioenergetics* **1847**: 931–938.

Ware MA, Belgio E, Ruban AV. 2015. Comparison of the protective effectiveness of NPQ in Arabidopsis plants deficient in PsbS protein and zeaxanthin. *Journal of Experimental Botany* **66**: 1259–1270.

Way DA, Pearcy RW. 2012. Sunflecks in trees and forests: from photosynthetic physiology to global change biology. *Tree Physiology* **32**: 1066–1081.

Wehner A, Grasses T, Jahns P. 2006. De-epoxidation of violaxanthin in the minor antenna proteins of photosystem II, lhcb4, lhcb5, and lhcb6. *Journal of Biological Chemistry* **281**: 21924–21933.

Wood WHJ, MacGregor-Chatwin C, Barnett SFH, Mayneord GE, Huang X, Hobbs JK, Hunter CN, Johnson MP. 2018. Dynamic thylakoid stacking regulates the balance between linear and cyclic photosynthetic electron transfer. *Nature Plants* **4**: 116–127.

Yamamoto H, Peng L, Fukao Y, Shikanai T. 2011. An Src homology 3 domain-like fold protein forms a ferredoxin binding site for the chloroplast NADH dehydrogenase-like complex in Arabidopsis. *Plant Cell* **23**: 1480–1493.

Yamamoto H, Shikanai T. 2019. PGR5-dependent cyclic electron flow protects photosystem I under fluctuating light at donor and acceptor sides. *Plant Physiology* **179**: 588–600.

Yamori W, Makino A, Shikanai T. 2016. A physiological role of cyclic electron transport around photosystem I in sustaining photosynthesis under fluctuating light in rice. *Scientific Reports* **6**: 20147.

Supporting Information

Additional Supporting Information may be found online in the Supporting Information section at the end of the article.

Notes S1 Introduction to frequency-domain analysis.

Notes S2 Raw ChlF yield data.

Notes S3 Influence of light history on the signal patterns.

Notes S4 ChlF yield data shown without separating the oscillatory and stationary components.

Please note: Wiley is not responsible for the content or functionality of any Supporting Information supplied by the authors. Any queries (other than missing material) should be directed to the *New Phytologist* Central Office.